Proc. Natl. Acad. Sci. USA
Vol. 96, pp. 11293–11298, September 1999
Biophysics

Evidence for the role of PrP^C helix 1 in the hydrophilic seeding of prion aggregates

M. P. MORRISSEY* AND E. I. SHAKHNOVICH†‡

*Division of Engineering and Applied Sciences, and †Department of Chemistry and Chemical Biology, Harvard University, 12 Oxford Street, Cambridge, MA 02138

Communicated by William Klemperer, Harvard University, Cambridge, MA, July 16, 1999 (received for review April 9, 1999)

ABSTRACT **Prions are mammalian proteins (PrPs) with a unique pathogenic property: a nonendogenous isoform PrP^{Sc} can catalyze conversion of the endogenous PrP^C isoform into additional PrP^{Sc}. In this work, we demonstrate that PrP^C helix 1 has certain properties (hydrophilicity, charge distribution) that make it unique among all naturally occurring α-helices, and which are indicative of a highly specific model of prion infectivity. The β-nucleation model proposes that PrP^{Sc} is an aggregate with a hydrophilic core, consisting of a β-sheet-like arrangement of constituent helix 1 components. It is suggested by using structural arguments, and confirmed by using CHARMM energy calculations, that aggregate formation from two PrP^C molecules is highly unfavorable, but the addition of chains to an existing aggregate is favorable. The β-nucleation model is shown to be consistent with the prion species-barrier, as well as with infectivity data. Sequence analysis of all known protein structures indicates that PrP is uniquely suited to β-nucleation, in contrast to the many proteins that readily form less favorable (often nonspecific) hydrophobic aggregates.**

Misfolded isoforms of the naturally occurring prion protein (PrP) have been shown to be the causative agents in a class of mammalian neurodegenerative disorders, including Creutzfeldt-Jakob disease (CJD) in humans, scrapie in sheep, and bovine spongiform encephalopathy (or "mad-cow disease") in cows (1). Prion infectivity is unique in that the pathogenic prion form (PrP^{Sc}) catalyzes the conversion of the endogenous form (PrP^C) into PrP^{Sc}, allowing a small infusion of pathogenic particles to "seed" the host for production of large amounts of the pathogenic form without the influence of foreign nucleic acids (1, 2). The so-called "protein-only" hypothesis asserts further that no extraneous agents are necessary to explain prions' unusual behavior; this hypothesis has been advanced by a number of *in vitro* experiments involving recombinant and synthetic prion fragments (2, 3).

The mechanism by which PrP^{Sc} can seed its host for further PrP^{Sc} production is unknown, although two major models have been proposed. The standard catalytic model (4) proposes that PrP^C and PrP^{Sc} are distinct monomeric stable states, with the presence of PrP^{Sc} catalyzing the conversion of PrP^C to PrP^{Sc}. The aggregative properties of PrP^{Sc} could be either incidental to or necessary for this conversion, and accessory molecules may or may not be necessary for conversion to PrP^{Sc} (5). Alternatively, the nucleated polymerization model (6, 7) proposes that PrP^{Sc} is intrinsically multimeric, differing from PrP^C primarily in quaternary structure. Changes in secondary and tertiary structure may accompany this change in polymerization state, as seems to occur with amyloid formation (8).

The structure of PrP^C has been determined by NMR to contain three α-helices (9, 10). Helix 1 spans residues 144–153, whereas helix 2 and helix 3 (residues 172–194 and 200–224, respectively) form a two-helix bundle. The N-terminal residues 1–91 are largely unstructured. The structure of PrP^{Sc} has not been elucidated, but is known to have significant β-sheet-like content (11).

Helix 1 Is Self-Stabilizing

PrP^C helix 1 (residues 144–153, see Fig. 1) is characterized by a highly unusual sequence that may play a pivotal role in prion infectivity. In proteins, α-helices and β-strands normally contain hydrophobic residues that form tertiary contacts with the protein core. Such interactions play a key role in stabilization of secondary structure (12, 13) and may be augmented by ion pairs (salt bridges) or disulfide bonds. PrP^C helix 1 breaks sharply with this conventional wisdom. First, it is composed entirely of hydrophilic residues (DWEDRYYREN), so it is not able to form stabilizing hydrophobic contacts with the protein core. Second, it is stabilized by two internal salt bridges, but makes no external (tertiary) salt bridges with the rest of the PrP^C molecule. Third, the ordering of charges interacts favorably with the intrinsic helix dipole moment.

To quantify the unusual hydrophilicity of PrP^C helix 1, we used the Database of Secondary Structure of Proteins (14) to extract all α-helices with eight or more residues from the Brookhaven Protein Data Bank (PDB) (15). (Structures that were complexes of proteins with other molecules were excluded.) There were 10,393 such helices. We then applied two hydrophilicity scales to each helix, taking the overall solubility of a helix to be the average of the hydrophilicities of its constituent residues. The results are stunning: using the hydrophilicity scale of Radzicka and Wolfendon (16), which was derived from experimental solubility data of individual amino acids, PrP^C helix 1 is the most soluble helix in the PDB. Fig. 2 presents a histogram of helix solubility data. Similarly, using the hydrophilicity scale of Kuhn *et al.* (17), which was derived from bound-water statistics in the PDB, prion helix 1 was the second most soluble of the 10,393 helices.

We see that PrP^C helix 1 has a remarkably low capacity to form tertiary hydrophobic interactions and must be stabilized instead by electrostatic interactions.

β-Nucleation

The sequence composition of PrP^C helix 1 also lends itself, however, to the formation of multichain aggregates that possess these same ionic interactions. One type of regular aggregate is the parallel β-sheetlike aggregate exemplified in Fig. 3. Fig. 3 *a* and *b* shows a two-chain instance of a parallel aggregate; salt bridges form between aspartic acid residues of one chain and arginine residues of its neighbor. The two-membered aggregate forms two salt bridges. Similarly, Fig. 3

The publication costs of this article were defrayed in part by page charge payment. This article must therefore be hereby marked "*advertisement*" in accordance with 18 U.S.C. §1734 solely to indicate this fact.

PNAS is available online at www.pnas.org.

Abbreviations: PrP, prion protein; CJD, Creutzfeldt-Jakob disease; PDB, Brookhaven Protein Data Bank.

‡To whom reprint requests should be addressed. E-mail: eugene@belok.harvard.edu.

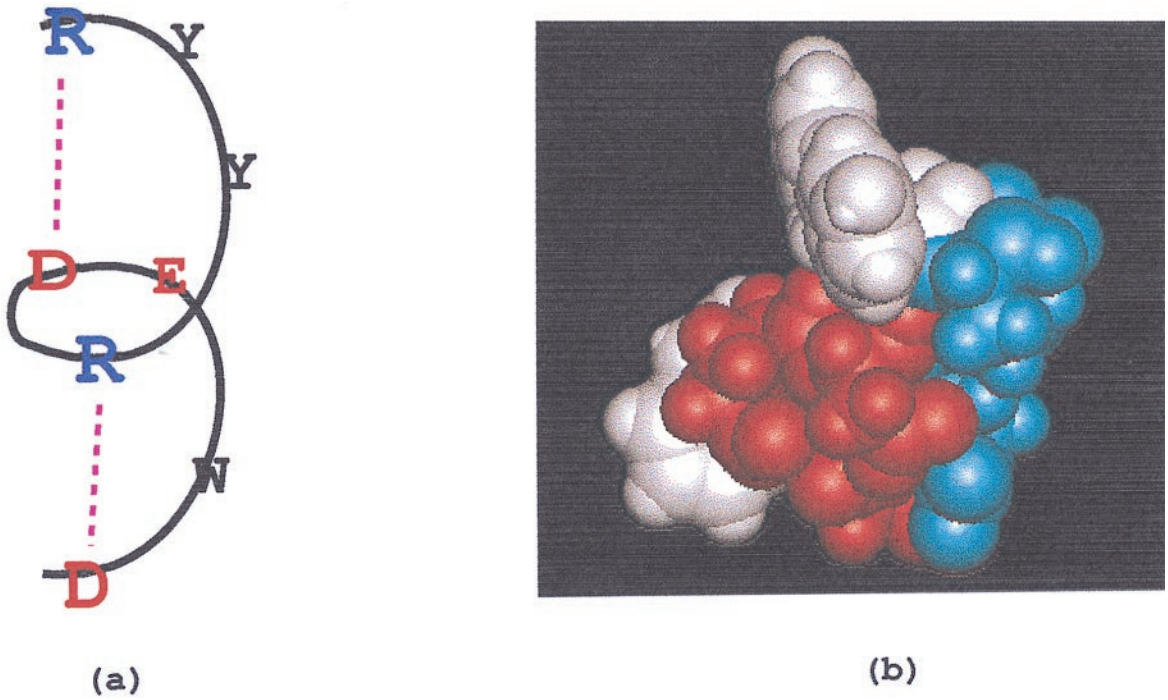

FIG. 1. (*a*) Schematic and (*b*) space-filling model of PrP^C helix 1 (first eight residues). Acidic residues (Asp and Glu) are colored red, while basic residues (arg) are blue. Each instance of helix 1 contains two Asp-Arg ion pairs (salt bridges), denoted by the dashed lines.

c and *d* shows a four-membered parallel aggregate, forming the same types of intermolecular ion pairs. The four-chain parallel β-aggregate forms six salt bridges.

In general, a parallel aggregate of N_C chains contains $2(N_C-1)$ salt bridges, in comparison to $2N_C$ salt bridges in N_C separate helices. Consequently, there is a penalty of two salt bridges for formation of the two-chain parallel aggregate, but no salt-bridge penalty for the addition of subsequent chains to the β-aggregate. Salt bridges are not the only energetic interactions in protein systems, but in a region of such extreme hydrophilicity as helix 1, with no potential for disulfide formation, salt bridges are likely to dominate energetically.

The β-nucleation model is a hybrid of the nucleated polymerization and catalytic models: we propose that PrP^{Sc} is fundamentally an aggregative state, but that a highly specific change in PrP^C structure, induced by PrP^{Sc}, is the key event in PrP^{Sc} propagation. Conversion to PrP^{Sc} is manifest as the unraveling of a PrP^C helix 1, followed by the addition of the residues of helix 1 to the core parallel aggregate. The effect of the helix 1 conformational change on the remaining PrP residues will be discussed below; for now, we concentrate on the helix 1 fragment in isolation.

Molecular Modeling Results

To test the β-nucleation model, we ran an exhaustive series of CHARMM (18) minimizations on the PrP^C helix 1 fragment. The results, which are presented in Table 1, also include identical tests on two control helices, which were chosen at random from the PDB (15). The control helices were GEQLGETL from PDB entry 1bia (19) (biotin operon repressor) and WDEAAVNLA from PDB entry 1lyd (20) (T4 lysozyme). Controls were run to demonstrate that the prion-like energetic behavior of PrP^C helix 1 is not an artifact of our minimization procedures or of the CHARMM molecular potential.

The first minimizations were run *in vacuo*. First, we calculated the minimized energy of the helix 1 fragment, DWEDRYYR, using the procedure described in Table 1. Next, we minimized three aggregates, with two, three, and four chains. The data was collated to represent the energetic penalty (reward) for three types of conformational transformations: (*a*) two helices unraveling to form a two-membered aggregate, (*b*) one helix unraveling to join an existing two-aggregate, forming a three-membered aggregate, and (*c*) one helix unraveling and joining a three-aggregate, to form a four-membered aggregate. We see that for PrP^C helix 1, there is a stiff penalty for the formation of a two-chain aggregate from two helices, caused in part by the reduction in the number of salt bridges. But after this point, the situation changes dramatically: adding more chains is energetically favorable. Importantly, the same phenomenon was not observed for the control helices. All energies presented are minimized enthalpies, considerably larger in magnitude than corresponding free energies. Enthalpy differences at 300 K were nearly identical to the minimized values. We expect free energy differences to take the same qualitative form as enthalpic data.

Next, we ran the same set of minimizations for a more realistic, fully solvated system. An ellipsoid of 900 water molecules was filled with the following combinations: (*a*) four α-helices, (*b*) two helices and a two-member β-aggregate, (*c*) one helix and a three-member β-aggregate, and (*d*) a four-member β-aggregate. All systems contained the same number of atoms, approximately 3,500. Minimizations were run as for the vacuum state, and the results are reported in Table 1. The solvated CHARMM results paint the same picture as the vacuum results: two PrP^C molecules face a huge barrier in forming a PrP^{Sc} β-nucleus, but once formed, the nucleus serves as a seed for the addition of additional PrP^C molecules to the aggregate. Once again, the control helices did not exhibit this distinctly prion-like behavior.

Note that to join a β-aggregate, helix 1 fragments must give up stabilizing PrP^C tertiary interactions. This additional energetic penalty also was calculated, and the results were as expected: the tertiary stabilizing energy for PrP^C helix 1 was minimal (enthalpy of less than 20 kcal/mol, meaning that addition of chains to an existing PrP^{Sc} β-aggregate is still highly favorable). The control helices, however, were stabilized by greater than 50 kcal/mol in tertiary interactions.

Discussion

The preceding CHARMM results support the assertion that the helix 1 region of PrP, via the β-nucleation mechanism, exhibits prion-like behavior. Conversion of PrP^{C} to PrP^{Sc}, or more specifically the unraveling of a PrP^{C} helix 1 and its addition to the PrP^{Sc} aggregate, is catalyzed by the very presence of PrP^{Sc}. Formation of PrP^{Sc} from PrP^{C} molecules alone is, as expected, prohibited by a large energetic barrier.

That the behavior of the helix 1 region is highly unusual, if not unique, is indicated by the highly unusual nature of PrP^{C} helix 1 itself, including (*a*) its extreme hydrophilicity, which excludes the possibility of tertiary stabilizing hydrophobic interactions, (*b*) the lack of tertiary salt bridges or disulfide bonds, and (*c*) the distribution of charges internal to helix 1. It also is anecdotally supported by CHARMM results on the two control helices, showing the lack of prion-like energetics for these sequences. The ability of PrP to form a tightly bound hydrophilic aggregate in aqueous solution is most unusual. That the aggregate's ordering makes its own initial formation prohibitively expensive (energetically), making the PrP sequence a unique candidate for "prion-like" behavior.

Although the helix 1 region seems to be crucial in determining prion behavior, the amyloid plaques associated with prion disease may still be largely hydrophobic aggregates. Notably, the precise fate of PrP helices 2 (residues 172–194) and 3 (residues 200–224), or of the hydrophobic region in the 110–120 region, is not directly addressed by the β-nucleation model, but may be important for the eventual formation of protease-resistant amyloidosis (21, 22). In particular, we note that in PrP^{C}, helix 2 and helix 3 form a two-helix bundle with a hydrophobic core; increases in the local concentration of these helices (via β-aggregation of helix 1 fragments from multiple chains) would allow the C-terminal region (spanning helix 2 and helix 3) to form a hydrophobic aggregate of 50+ residues per participating PrP molecule. A similar phenomenon is possible involving aggregation of the region preceding helix 1. Thus it is proposed that while the helix 1 residues do not form the primary mass of amyloid deposits, they enable the formation of amyloid indirectly by increasing the local concentration of the hydrophobic regions of PrP. There are a number of experiments in the literature that allude to the importance of the helix 1 residues in forming intermolecular interactions; three of these will be discussed now.

Comparison with Experiment

The primary role of helix 1-charged residues in intermolecular interactions is bolstered by data reported by Sharman *et al.* (23), who performed CD and NMR studies of three peptides selected from PrP. Interestingly, fragments 125–170 and 142–170 required a buffer pH of 3.0 (below the pKa of aspartic and glutamic acids) to maintain solubility, whereas region 156–170 (the only fragment that does not span helix 1) remained soluble at pH 4.5. Paradoxically, at pH values above 4.5, the most hydrophilic helix in the PDB seems responsible for aggregation-driven insolubility.

Fig. 4 illustrates an antiparallel two-chain aggregate of helix 1 residues that may be responsible for the poor solubility of helix 1 fragments noted in ref. 23. The antiparallel aggregate is unlikely to grow beyond two chains because of side-chain constraints. Although antiparallel aggregation is structurally distinct from the parallel β-nucleation aggregates, both models

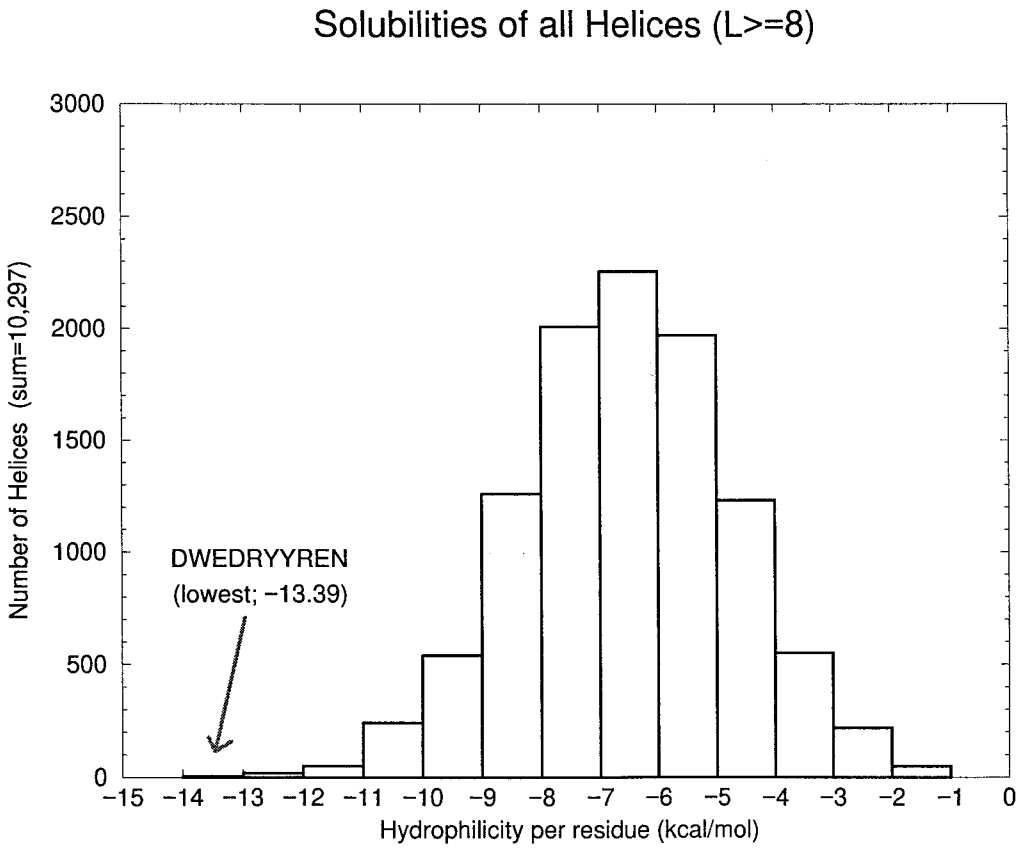

FIG. 2. Hydrophilicities of all 10,363 α-helices (with $\geq$eight residues, taken from proteins and partial proteins with $\geq$20 residues) in the PDB (15). Helix solubility is taken as the average hydrophilicity of the amino acids comprising the helix. We use the scale of Radzicka and Wolfendon (16). It is notable that the most hydrophilic known, naturally occurring α-helix is PrP^{C} helix 1, and that this helix stabilizes itself by means of internal salt bridges rather than by tertiary hydrophobic interactions.

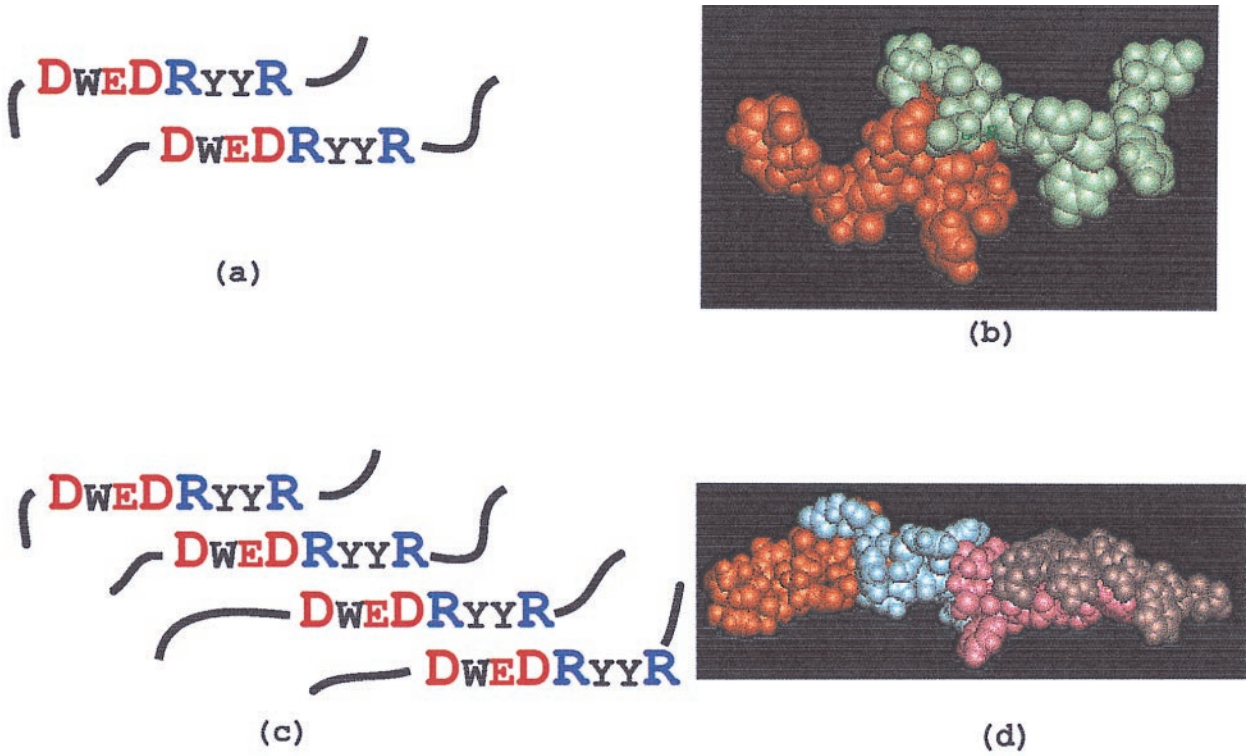

FIG. 3. PrP and the β-nucleation model. (*a*) Schematic and (*b*) minimized space-filling model of a two-membered β-aggregate, comprised of residues 144–151 from two separate PrP molecules. The aggregate contains two Asp-Arg salt bridges (ion pairs). (*c*) Schematic and (*d*) minimized space-filling model of a four-membered aggregate. The four-membered aggregate contains six Asp-Arg salt bridges. A parallel aggregate of arbitrary number of chains N_C would contain $2(N_C-1)$ such salt bridges, whereas N_C separate helix 1 fragments contain $2N_C$ salt bridges.

rely on the formation of intermolecular Asp-Arg salt bridges in the ultra-hydrophilic helix 1 region.

The β-nucleation model clarifies an aspect of PrP^{Sc} behavior observed *in vitro* by Kocisko *et al.* (24). Those authors demonstrated that the transforming ability of PrP^{Sc} is restored after temporary treatment with 3 M GdHCl, but is lost permanently at higher denaturant concentration. In 3 M GdHCl, PrP^{Sc} fragments marked by an epitope at residues 143–156 remained protease resistant, whereas fragments marked by other epitopes (residues 90–115 and 217–232) were susceptible to proteolysis. This finding indicates that stability of PrP^{Sc} in the region 143–156 (corresponding to PrP^{C} helix 1) is correlated with retention of infectivity in direct accordance with the β-nucleation model. At higher denaturant concentration, the 143–156 fragment is dissolved into monomeric form, restoring the free energy barrier to PrP^{Sc} formation and resulting in irreversible loss of infectivity.

A third interesting result was presented by Muramoto *et al.* (22), who created a recombinant PrP^{C}, termed $PrP^{C}-106$, by deleting a 36-residue span from the natural variant. This excised region spanned residue 141–176, which included helix 1. The authors found that the mutant peptide became protease resistant (this form was named $PrP^{Sc}-106$) in the presence of natural PrP^{Sc}. Additionally, it was found that $PrP^{Sc}-106$ is soluble under certain conditions, showing that aggregation and protease resistance are separable for this system. (Solubility is taken as a proxy for the availability of the substance in a single-molecule form.) At first glance, this would seem to indicate that (*a*) prion conversion is not fundamentally an aggregative process, and (*b*) the excised region (and thus helix 1) play no important role in prion behavior. On closer inspection, however, Muramoto's experiments may indicate just the opposite.

Notably, Muramoto *et al.* did not attempt a structural characterization of $PrP^{C}-106$. Because many of the deleted

Table 1. Thermodynamic data supporting the β-nucleation mechanism

	Vacuum ΔE, kcal/mol			Solvated ΔE, kcal/mol		
	PrP	Control 1	Control 2	PrP	Control 1	Control 2
Two helices ⇒ two-aggregate	+67	+79	+142	+373	+110	+199
Two-aggregate + one helix ⇒ three-aggregate	−57	+90	+121	−184	+27	+21
Three-aggregate + one helix ⇒ four-aggregate	−31	+98	+43	−156	+57	+44

ΔE represents the energy difference for transformation of one state to another (e.g., two helices to a two-membered aggregate). A series of CHARMM Newton-Raphson minimizations were performed on various numbers and conformations of helix 1 fragments. We began each calculation from a state with the appropriate gross features (i.e., four parallel fragments in a sheetlike arrangement) and minimized the energy of this system. The system then was repeatedly heated to 400 K and reminimized until the minimized energy was reproducible, and thus taken as a "global" minimum. Minimizations were first run *in vacuo*, and then for corresponding systems solvated in a large aqueous ellipsoid, with a fixed number of solvent atoms (approximately 2,700). We ran each set of experiments for the PrP helix 1 fragment as well as for two control helices chosen randomly from the PDB. [The control helices were GEQLGETL from PDB entry 1bia(19) and WDEAAVNLA from PDB entry 11yd(20).] In both the vacuum and solvated cases, the results support the β-nucleation hypothesis: formation of the two-membered parallel aggregate is prohibitively expensive, while addition of helix 1 fragments to an existing aggregate is energetically favorable. The controls demonstrated that this property is not an artifact of our methodology or of the CHARMM force field.

FIG. 4. Two-membered antiparallel aggregate, which maintains the four salt bridges of its two helix 1 predecessors and should form more readily than the two-chain parallel aggregate. However, there is no mechanism for further growth.

residues participate in the PrP^C protein core, and the two ends that were sewn together (residues 140 and 177) are maximally separated in native PrP^C (30), it is unlikely that PrP^C-106 bears much structural resemblance to naturally occurring PrP^C. Indeed, it is unclear that PrP^C-106 even has a unique folded state, given that much less intrusive mutations are often catastrophically destabilizing (25, 26). Additionally, although the authors were able to solubilize $PrP^{Sc}-106$ under certain conditions, there has been no indication in the literature that native PrP^{Sc} is soluble; at the time of this writing, natural PrP^{Sc} has not been isolated in monomeric form. Thus the separability of protease resistance from aggregation for $PrP^{Sc}-106$ does not indicate the same separation for natural PrP^{Sc}.

As a further step, we scanned the PDB (15) for all 36-residue windows in known structures and found that the only one in 2,600 36-residue spans (0.038 percent) is more hydrophilic than the region deleted to make PrP−106. It is certainly interesting that PrP^{Sc} could induce protease resistance in PrP^C-106, possibly by allowing the poorly structured peptide to form a hydrophobic core. But if $PrP^{Sc}-106$ bears any resemblance to native PrP^{Sc}, as the authors suggest, it would be difficult to reconcile how deleting an extremely hydrophilic span could make in insoluble protein soluble. This result would be predicted by the β-nucleation model, however, in which hydrophilic residues bear primary responsibility for tight aggregation.

CJD and the Prion Species Barrier

Several types of mutations may result in CJD, which is characterized by the spontaneous formation of PrP^{Sc} (as distinct from scrapie and bovine spongiform encephalopathy, which require the infectious introduction of PrP^{Sc}). The most commonly noted is an insertion in the octapeptide repeat region of the unstructured N terminus (27, 28). Although this is far (in sequence) from helix 1, it should be noted that (*a*) prion infectivity has been achieved by using PrP^{Sc} regions stripped of the octapeptide region altogether (29) and (*b*) other mutations throughout the PrP molecule also have been implicated in CJD (30). Thus it is likely that CJD-causing mutations work by an indirect mechanism to promote PrP^{Sc} formation.

Recent studies of amyloid fibrils have shown that destabilizing tertiary contacts relative to intrahelical contacts accelerates amyloid formation (31, 32). In this light, CJD mutations may further weaken helix 1's already slight tertiary interactions. Insertions in the unstructured C-terminal region certainly would be capable of such destabilization, as would point mutations in regions adjacent to helix 1.

Finally, we note that the β-nucleation model is markedly consistent with species barrier data in the literature. There are four residues within or in direct contact with helix 1, which are variable among mammalian species: residues 139, 143, 145, and 155. (Sequence data were obtained from the SWISS-PROT database; ref. 33.) All other residues from 125–163 are conserved. Categorizing by sequence homology yields five major groups: (*a*) monkeys, baboons, cats, camels, rabbits, goats, and sheep, (*b*) humans, cows, gorillas, and chimps, (*c*) mice, (*d*) hamsters, and (*e*) rats. Based on these groupings, one would predict a species barrier between cows and sheep, cows and monkeys, hamsters and mice, etc. All are well established in the literature (34), but in each case there are other mutations in PrP, away from helix 1, which also could contribute to the species barrier. Based on mutations of residues contacting helix 1, the β-nucleation model predicts no species barrier between sheep and monkeys, however, despite several sequence differences distant from helix 1. Baker *et al.* (35) demonstrated recently through clinical and pathologic experiment that this is indeed the case. Additionally, residues 139, 155, and 170 have been determined to be the critical residues in the mouse-hamster barrier (36–38); residues 139 and 155 are both in direct contact with helix 1.

Conclusion

Following the elucidation of the hypersolubility and unusual charge structure of PrP^C helix 1, we have proposed a model of prion infectivity and PrP^{Sc} structure based largely on the properties of this helix. The β-nucleation model states that although the tertiary structures of PrP^C and PrP^{Sc} differ markedly, the pathogenic isoform PrP^{Sc} is fundamentally a highly specific hydrophilic aggregate. β-nucleation provides an explanation of prion infectivity, in a manner consistent with *in vitro* and *in vivo* experiments, and with observations of the prion species barrier.

Note Added in Proof. After this paper was in proofs, it was noted that the salt bridge 151R-152E can form in place of the 147D-151R salt bridge shown in Fig. 1*a*. The two helix conformers have similar CHARMM energetics. For completeness, all of the CHARMM minimizations in this paper were rerun for the complete helix 1 (DWEDRYYREN) rather than for the eight-residue fragment (DWEDRYYR) reported in the text. The data corresponded very closely to that in Table 1, preserving the large barrier of aggregate formation and a similar favorability of aggregate growth.

We thank Peter Lansbury, Byron Caughey, Sung Choe, Jun Shimada, and Gabriel Berriz for many interesting comments, discussions, and suggestions. This work was supported by National Institutes of Health Grant GM52126.

1. Prusiner, S. B. (1997) *Science* **278**, 245–251.
2. Harrison, P. M., Bamborough, P., Daggett, V., Prusiner, S. B. & Cohen, F. E. (1997) *Curr. Opin. Struct. Biol.* **7,** 53–59.
3. Kaneko, K., Wille, H., Mehlhorn, I., Zhang, H., Ball, H., Cohen, F. E., Baldwin, M. A. & Prusiner, S. B. (1997) *J. Mol. Biol.* **270,** 574–586.
4. Huang, Z., Prusiner, S. B. & Cohen, F. E. (1996) *Folding Des.* **1,** 13–19.
5. Telling, G. C., Scott, M., Mastrianni, J., Gabizon, R., Torchia, M., Cohen, F. E., DeArmond, S. J. & Prusiner, S. B. (1995) *Cell* **83,** 79–90.
6. Lansbury, P. T. & Caughey, B. (1995) *Chem. Biol.* **2,** 1–5.
7. Caughey, B., Kocisko, D. A., Raymond, G. J. & Lansbury, P. T. (1995) *Chem. Biol.* **2,** 807–816.
8. Kelly, J. W. (1998) *Curr. Opin. Struct. Biol.* **8,** 101–106.
9. Riek, R., Hornemann, S., Wider, G., Billeter, M., Glockshuber, R. & Wuthrich, K. (1996) *Nature (London)* **382,** 180–182.
10. James, T. L., Liu, H., Ulyanov, B., Farr-Jones, S., Zhang, H., Donne, D. G., Kaneko, K., Groth, D. & Mehlhorn, I. (1997) *Proc. Natl. Acad. Sci. USA*, **94,** 10086–10089.
11. Nguyen, J., Baldwin, M. A., Cohen, F. E. & Prusiner, S. B. (1995) *Biochemistry* **34,** 4186–4192.
12. Minor, D. L. & Kim, P. S. (1994) *Nature (London)* **371,** 264–267.
13. Minor, D. L. & Kim, P. S. (1996) *Nature (London)* **380,** 730–734.
14. Kabsch, W. & Sander, C. (1983) *Biopolymers* **22,** 2577–2637.
15. Abola, E. E., Sussman, J. L., Prilusky, J. & Manning, N. O. (1997) in *Methods in Enzymology*, eds. Carter, C. W. & Sweet, R. M. (Academic, San Diego), pp. 556–571.

16. Radzicka, A. & Wolfenden, R. (1988) *Biochemistry* **27,** 1664–1670.
17. Kuhn, L. A., Swanson, C. A., Pique, M. E., Tainer, J. A. & Getzoff, E. D. (1995) *Proteins Struct. Funct. Genet.* **23,** 536–547.
18. Mackerell, A. D., Bashford, D., Dunbrack, R. L., Field, M. J., Gao, J., Ha, S., Bellott, M., Evanseck, J. D., Fischer, S. & Guo, H. (1998) *J. Phys. Chem. B* **102,** 3586–3616.
19. Wilson, K. P., Shewchuk, L. M., Brennan, R. G. & Otsuka, A. J. (1992) *Proc. Natl. Acad. Sci. USA* **89,** 9257–9261.
20. Rose, D. R., Phipps, J., Michniewicz, J., Birnbaum, G. I., Ahmed, F. R., Muir, A., Anderson, W. F. & Narang, S. (1988) *Protein Eng.* **2,** 277–181.
21. Chabray, J., Caughey, B. & Chesebro, B. (1998) *J. Biol. Chem.* **273,** 13203–13207.
22. Muramoto, A. Scott, M., Cohen, F. E. & Prusiner, S. B. (1996) *Proc. Natl. Acad. Sci. USA* **93,** 15457–15462.
23. Sharman, G. J., Kenward, N., Williams, H. E., Landon, M., Mayer, R. J. & Searle, M. S. (1998) *Folding Des.* **3,** 313–320.
24. Kocisko, D. A., Lansbury, P. T. & Caughey, B. (1996) *Biochemistry* **35,** 13434–13442.
25. Mateu, M. & Fersht, A. (1998) *EMBO J.* **17,** 2749–2758.
26. Tissot, A. C., Vuilleumier, S. & Fersht, A. R. (1996) *Biochemistry* **35,** 6786–6794.
27. Goldfarb, L. G., Brown, P., McCombie, W. R., Goldgaber, D., Swergold, G. D., Wills, P. R., Cervenakova, L., Baron, H., Gibbs, C. J. & Gajdusek, D. C. (1991) *Proc. Natl. Acad. Sci. USA* **88,** 10926–10930.
28. Krakauer, D. C., Zanotto, P. M. & Pagel, M. (1998) *J. Mol. Evol.* **47,** 133–145.
29. Prusiner, S. B., Bolton, D. C., Groth, D. F., Bowman, K. A., Cochran, S. P. & McKinkey, M. P. (1982) *Biochemistry* **21,** 6942–6950.
30. Priola, S. A. & Chesebro, B. (1998) *J. Biol. Chem.* **273,** 11980–11985.
31. Chiti, F., Webster, P., Taddei, N., Clark, A., Stefani, M., Ramponi, G. & Dobson, C. M. (1999) *Proc. Natl. Acad. Sci. USA* **96,** 3590–3594.
32. Grob, M., Wilkins, D. K., Pitkeathly, M. C., Chung, E. W., Higham, C., Clark, A. & Dobson, C. M. (1999) *Protein Sci.* **8,** 1350–1357.
33. Bairoch, A. & Apweiler, R. (1999) *Nucleic Acids Res.* **27,** 49–54.
34. Billeter, M., Riek, R., Wider, G., Hornemann, S., Glockschuber, R. & Wuthrich, K. (1997) *Proc. Natl. Acad. Sci. USA* **94,** 7281–7285.
35. Baker, H. F., Ridley, R. M., Wells, G. A. & Ironside, J. W. (1998) *Neuropathol. Appl. Neurobiol.* **24,** 476–486.
36. Kocisko, D. A., Priola, S. A., Raymond, G. J., Lansbury, P. T. & Caughey, B. (1995) *Proc. Natl. Acad. Sci. USA* **92,** 3923–3927.
37. Priola, S. A. & Chesebro, B. (1995) *J. Virol.* **69,** 7754–7758.
38. Scott, M., Foster, D., Mirenda, C., Serban, D., Coufal, F., Walchli, M., Torchia, M., Groth, D., Carlson, G., Dearmond, S. J., *et al*. (1989) *Cell* **59,** 847–857.